International Journal for Housing Science and Its Applications
Publish August 6, 2025. Volume 46, Issue 3 Pages 7720-7730

https://doi.org/10.70517/ijhsa463662

Research on Intelligent Weather Forecasting Based on Cloud Radar and Weather Sensor Data Fusion

Yaping Fu[1], Fang Li[2,*], Yuanxin Fu[2], Bin Wen[3], Jingjing Li[1], Zichen Pei[1] and Chen Zhao[1]
[1] Shanxi Provincial Atmospheric Detection Technology Support Center, Taiyuan, Shanxi, 030002, China
[2] Shanxi Province Meteorological Society, Taiyuan, Shanxi, 030002, China
[3] Chengdu University of Information Technology, Chengdu, Sichuan, 610200, China
Corresponding authors: (e-mail: 13935165093@163.com).

Abstract With the continuous development of weather prediction technology, the traditional single data source prediction model has been difficult to meet the demand of increasingly complex weather changes. In this paper, an intelligent weather prediction model based on the fusion of cloud radar and weather sensor data is proposed, which utilizes a combination of Kalman filter algorithm and deep learning model for weather forecasting. First, the Kalman filter algorithm is used to invert the cloud radar echo data, and the inversion accuracy is improved by optimizing the parameters, with the lowest temperature deviation reaching 3.2 K. Then, based on the multimodal fusion of weather prediction model, the temporal and spatial dependencies in the meteorological data are modeled using the Transformer encoder-decoder architecture, which further improves the prediction accuracy. The experimental results show that the model in this paper performs better in the evaluation indexes of RMSE, MSE and MAPE compared with the LSTM and RNN models, with an RMSE of 2.6483, a MAPE of 0.0229, and an R^2 value close to 1, which makes the prediction results the closest to the real values. The model shows significant advantages in multimodal data fusion and provides an effective solution in the field of weather prediction.

Index Terms cloud radar, Kalman filter, deep learning, multimodal fusion, weather prediction, Transformer

I. Introduction

Weather forecasting is a central means for humans to cognize weather changes and reduce the risk of natural disasters [1]. However, the complexity of weather changes makes the current weather forecast accuracy still has many shortcomings [2]. Traditional weather forecasting models use basic observation data and empirical models to calculate forecasts, and with the development of science and technology, weather forecasts are gradually intelligentized [3]-[5]. Some emerging technologies such as artificial intelligence, internet of things, and cloud computing have brought many powerful tools and algorithms for weather forecasting, which not only improve the forecasting accuracy, but also make the forecasting work faster and more efficient, especially the cloud radar and weather sensor data fusion of intelligent weather forecasting has been widely used in recent years [6]-[9].

Cloud radar is a device that detects cloud structure, water vapor distribution, and precipitation processes by transmitting radio waves [10]. This technology can monitor the internal changes of cloud bodies in real time, help people to know the weather trends in advance, and is widely used in many fields [11], [12]. In contrast, weather sensor is a device that measures and monitors the parameters of the atmospheric environment, which is widely used in the fields of meteorology, climate research, weather forecasting, and agricultural production [13], [14]. Compared with the traditional weather forecasting methods, the intelligent weather forecasting by fusion of cloud radar and weather sensor data can deal with more complex information, including massive meteorological data, artificial satellite data, geographic information, wind sensors and other data sources [15]-[18]. Meanwhile, it can also improve the accuracy of the forecast by self-adjustment through data analysis and learning [19]. In addition, meteorological data can be quickly processed and analyzed to provide real-time and accurate forecasting information [20], [21]. Intelligent weather forecasting based on the fusion of cloud radar and weather sensor data has an important application value in natural disasters, aerospace, transportation, and other occasions where timely processing of weather information is required [22]-[24].

With global climate change and frequent meteorological disasters, weather forecasting plays an increasingly important role in disaster prevention and mitigation. Traditional weather prediction models usually rely on a single data source, which is difficult to comprehensively reflect complex weather trends. The fusion of cloud radar and weather sensors, on the other hand, can provide more multi-dimensional meteorological data and provide more comprehensive information for prediction models. Therefore, the development of meteorological prediction models based on multimodal data fusion has become an important direction to improve prediction accuracy.

The Kalman filter algorithm has become a commonly used tool in meteorological data processing due to its efficiency and accuracy in processing linear systems. However, the traditional Kalman filter algorithm often has certain limitations when dealing with nonlinear meteorological data, especially when dealing with complex meteorological systems, the stability and prediction accuracy of the algorithm are insufficient. For this reason, this paper proposes a meteorological prediction framework based on the combination of Kalman filtering and deep learning modeling, which aims to overcome the shortcomings of traditional filtering algorithms through deep learning techniques.

In this study, the Kalman filter algorithm is first used to preprocess the cloud radar echo data, and the inversion accuracy is further improved by improving the algorithm. Then, the multimodal data fusion method is used to model the spatio-temporal features of the meteorological data by combining the Transformer model in deep learning. Through the adaptive property of deep learning, the complex patterns and changing trends in meteorological data can be better captured. Finally, the prediction performance of this paper's model is evaluated through comparative experiments, which verifies its advantages in weather prediction.

II. Research on intelligent weather forecasting models

In this paper, Kalman filtering algorithm is used to apply in the study of cloud radar weather prediction, and combined with the constructed multimodal fusion weather prediction model to jointly realize the weather forecast.

II. A. Sensor data processing based on Kalman filter algorithm

Kalman filtering algorithm is a linear filtering recursive algorithm. The algorithm uses a set of recursive formulas to solve the filtering equations consisting of state equations and measurement equations. By modifying the important parameters in the recursive system, using the prediction error of the previous moment to feed back to the original prediction equation, and correcting the coefficients of the prediction equation in a timely manner, the optimal filter value for the next moment can be repeatedly recursively calculated [25]. Because the algorithm is very easy for computers to process, and has the characteristics of using recursive methods to solve the linear filtering problem. Therefore, the Kalman filter algorithm has been generally welcomed and has been widely used in the fields of econometrics, inertial guidance systems, radar trackers, satellite navigation systems, and dynamic positioning systems.

With the development of computer technology, the numerical stability, computational efficiency, algorithmic utility and effectiveness of the Kalman filter algorithm began to slowly fail to keep up with the requirements of computing. In order to improve the numerical stability and computational efficiency of the Kalman filter algorithm, a series of robust filtering algorithms have been proposed on the basis of the original Kalman filter algorithm. For example, the extended Kalman filter [26], the trace-free Kalman filter [27], and so on.

II. A. 1) Principles of Kalman filtering algorithm

Assume that the state and measurement equations of the system are, respectively:

$$X_K = \Phi_{K,K-1} X_{K-1} + \Gamma_{K,K-1} W_{K-1} \tag{1}$$

$$Z_K = H_K X_K + V_K \tag{2}$$

In the above equation, X_K is the state of the system at the moment K, $\Phi_{K,K-1}$ and $\Gamma_{K,K-1}$ are the state transfer matrices from the moment $K-1$ to the moment K, Z_K is the measurement value at the moment K, H_K is the parameter of the measurement system, W_K and V_K denote the process noise and observation noise, which are assumed to be Gaussian white noise. If the estimated state and observation satisfy Eq. (1), and the system process noise and observation noise satisfy the assumptions of Eq. (2), the estimate $\hat{X}$ of the observation X_K at moment K can be solved by the following equation.

State one-step prediction:

$$\hat{X}_{K,K-1} = \Phi_{K,K-1} \hat{X}_{K-1} \tag{3}$$

State Estimation:

$$\hat{X}_k = \hat{X}_{K,K-1} + K_K [Z_K H_K \hat{X}_{K,K-1}] \tag{4}$$

Filter gain matrix:

$$K_K = P_{K,K-1} H_K^T R_K^{-1} \tag{5}$$

One-step prediction error variance array:

$$P_{K,K-1} = \Phi_{K,K-1} P_{K-1} \Phi_{K,K-1}^T + \Gamma_{K,K-1} Q_{K-1} \Gamma_{K,K-1}^T \tag{6}$$

Estimating the error variance array:

$$P_K = \left[I - K_K H_K \right] P_{K,K-1} \tag{7}$$

Given the initial values X_0 and P_0, and based on the observations Z_K at K moments, the state estimates $\hat{X}_K \left(K = 1, 2, \cdots, N \right)$ at K moments can be calculated recursively.

Finally, the state estimates can be obtained by applying Eqs. (1) to (7) recursively with the given initial values and the observed values obtained from the observations.

II. A. 2) Algorithm improvements and applications

In order to improve the problem of poor estimation effect in Kalman filtering, this paper proposes the following improvement ideas:

(1) Pre-complete offline a large number of complex Kalman filter gain and error calculations in the calculation process of the Kalman filter algorithm.

(2) Replace the state equation of the estimated state of the system $\hat{S}$ in the Kalman filtering algorithm by the multiplication of matrix and volume vector.

Assume that the state equation of the estimated state S_k of the system at moment k is described as follows:

Observation equation:

$$U_k = H_k S_k + v_k \tag{8}$$

Equation of state:

$$\hat{S}_k = \hat{S}_{k-1} + K_k (A - H_k \hat{S}_{k-1}) \tag{9}$$

One-step prediction error variance array:

$$P_{1k} = \Phi_k P_{k-1} \Phi_k^T + \Gamma_k Q_{k-1} \Gamma_k^T \tag{10}$$

Filter gain matrix:

$$K_k = P_{1k} H_k^T (H_k P_{1k} H_k^T + R_k)^{-1} \tag{11}$$

Estimating the error variance array:

$$P_k = (I - K_k H_k) P_{1k} \tag{12}$$

where Φ_k is the one-step transfer matrix at moment $t(k)$, Γ_k is the system noise matrix, U_k is the system observation that can be obtained directly, H_k is the system observation matrix, and v_k is the observation noise of the system.

It is obtained after improvement:

$$P_{1k} = \Phi_k (P_{1k-1} - K_{k-1} H_{k-1} P_{1k-1}) \Phi_k^T + \Gamma_k Q_{k-1} \Gamma_k^T \tag{13}$$

$$\hat{S}_k = Y_k \hat{S}_{k-1} + K_k U_k \tag{14}$$

where $Y_k = E_k - H_k K_k$. If frequency determination is used, each element of Y_k and K_k is constant. Eq. (14) consists of the multiplication operation of 2 matrices and 1 column vector, so a large number of complex Kalman filtering gains and coefficients can be completed offline in advance, which greatly reduces the amount of arithmetic and improves the algorithm estimation accuracy, which can meet the requirements of practical applications. The Kalman filter algorithm improvement process is shown in Figure 1.

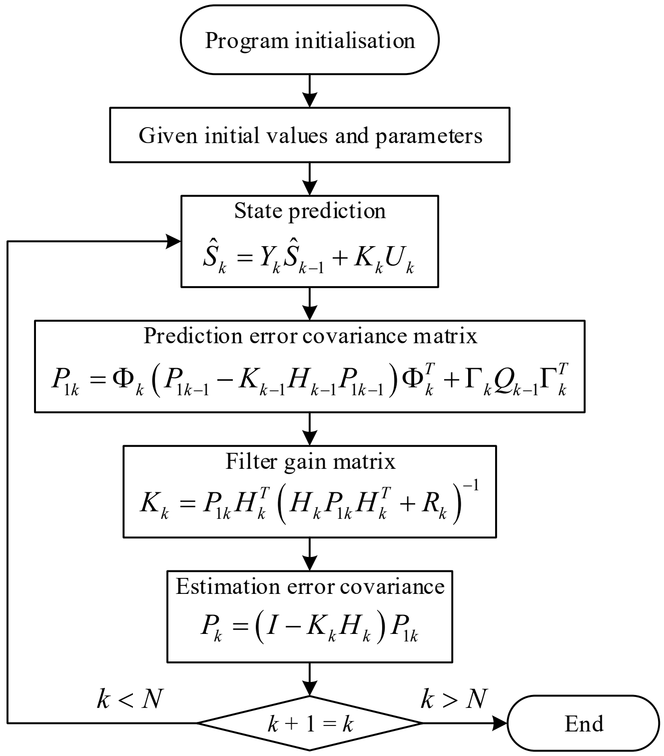

Figure 1: Kalman filtering improved algorithm process

II. B. Weather prediction model construction with multimodal fusion

II. B. 1) Model Architecture

The task of weather prediction can be formulated as a sequence prediction problem. Specifically, given a historical sequence of meteorological observations $X = \left\{ M^{t-T_{in}+1}, M^{t-T_{in}+2}, \cdots, M^t \right\}$, the meteorological data for the future time period is predicted $\hat{Y} = \left\{ \hat{M}^{t+1}, \hat{M}^{t+2}, \cdots, \hat{M}^{t+T_{out}} \right\}$. Where T_{in}, T_{out} denote the sequence length of input and the sequence length of output, respectively. The goal of this paper is to construct a deep learning model that makes the prediction sequence $\hat{Y}$ close to the real weather observation data $Y = \left\{ M^{t+1}, M^{t+2}, \cdots, M^{t+T_{out}} \right\}$.

Based on the above representation, the weather prediction task can be formulated as a sequence prediction problem. Specifically, given a historical sequence of meteorological observations $X = \left\{ M^{t-T_{in}+1}, M^{t-T_{in}+2}, \cdots, M^t \right\}$, the forecasting of meteorological data for the future time period $\hat{Y} = \left\{ \hat{M}^{t+1}, \hat{M}^{t+2}, \cdots, \hat{M}^{t+T_{out}} \right\}$. Where T_{in}, T_{out} denote the sequence length of input and the sequence length of output, respectively. The goal of this paper is to construct a deep learning model that makes the predicted sequence $\hat{Y}$ close to the real meteorological observation data $Y = \left\{ M^{t+1}, M^{t+2}, \cdots, M^{t+T_{out}} \right\}$.

Overall, the model proposed in this paper consists of three parts: a multimodal feature fusion network, a Transformer-based encoder-decoder network and a spatial regression network, and the overall framework of the model is shown in Fig. 2. The multimodal fusion network utilizes a convolutional network to extract the spatial features of the sequence data while fusing the multimodal features. Notation F^t denotes the feature map of the meteorological data at the moment of t through the multimodal fusion network. Based on the multimodal feature fusion, the Transformer encoder-decoder structure further models the spatial and temporal dependencies among the meteorological data. The decoder outputs the final feature representation $\left\{ Z^{t+1}, Z^{t+2}, \cdots, Z^{t+T_{out}} \right\}$. Finally, the spatial regression network converts the spatio-temporal feature maps output from the decoder into the final predictions $\left\{ \hat{M}^{t+1}, \hat{M}^{t+2}, \cdots, \hat{M}^{t+T_{out}} \right\}$.

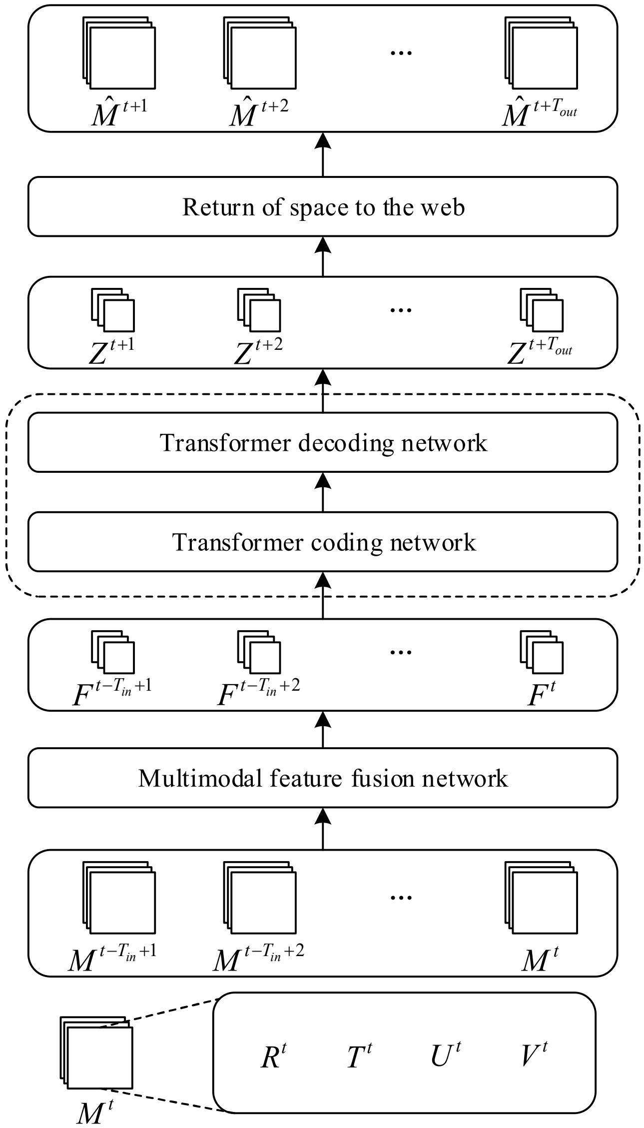

Figure 2: Overall framework of model

II. B. 2) Multimodal feature fusion networks

In order to learn the coupling relationship between different modes (humidity, temperature, latitudinal wind speed and meridional wind speed), and at the same time to effectively fuse the multimodal features, a multimodal feature fusion network is designed in this paper, which is characterized by the following main features:

(1) Structurally, a multi-branch hierarchical fusion strategy is adopted.

(2) Technically, a feature fusion method based on a gating mechanism is used. The input of each layer in the fusion branch contains the current features R_j^t, T_j^t, U_j^t, V_j^t of each modal branch, and the current fusion feature F_j^t, and the initial fusion feature is set to zero:

$$G_j^F, G_j^R, G_j^T, G_j^U, G_j^V = \sigma\left(M_{\theta_j}\left(F_j^t, R_j^t, T_j^t, U_j^t, V_j^t\right)\right) \tag{15}$$

$$F_{j+1}^t = G_j^F \otimes F_j^t + G_j^R \otimes R_j^t + G_j^T \otimes T_j^t + G_j^U \otimes U_j^t + G_j^V \otimes V_j^t \tag{16}$$

where G_j^R, G_j^T, G_j^U, G_j^V denote the corresponding gating weights of each modality, and G_j^F denotes the gating weights of the current multimodal fusion feature. In addition, σ denotes the Sigmoid function, which is a commonly used gating activation function. $\otimes$ denotes the Hadamard product. M_{θ_j} is the gating generation network.

II. B. 3) Transformer-based encoder-decoder network

Based on the spatial features extracted from the multimodal fusion network, the spatio-temporal dependencies between the data are further learned by the Transformer encoder-decoder [28]. The attentional mechanism is at the heart of the Transformer model and can be described as the process of mapping a query and a set of “key-value pairs” to an output. Given a set of query matrices $Q \in \mathbb{R}^{N_q \times d}$, and key-value matrices $K, V \in \mathbb{R}^{N_k \times d}$, the output of the attentional operation is as follows:

$$Attention(Q,K,V) = soft\max\left(\frac{QK^T}{\sqrt{d}}\right)V \tag{17}$$

When $Q = K = V$, it is called a self-attention mechanism. Multi-attention is an extension of the attention mechanism that runs k attention operations in parallel by projecting queries, keys, and values to different subspaces via a learnable k set of linear transformations. The outputs of these k attentions are then spliced together to obtain the final output via a learnable linear transformation:

$$MultiHeadAttention(Q,K,V) = Concat(h_1, h_2, \cdots, h_k)W^O \tag{18}$$

$$h_i = Attention\left(QW_i^Q, KW_i^K, VW_i^V\right) \tag{19}$$

where $W_i^Q, W_i^K, W_i^V \in \mathbb{R}^{d \times d_h}$ are the parameter matrices of the linear transformations of queries, keys, and values, respectively, and $W^O \in \mathbb{R}^{kd_h \times d}$ is the multicentered attention mechanism's final parameter matrix of the linear transformation. In general, d_h is often set to d/k.

After the attention operation the features still maintain the global receptive field, and the axial attention output $\tilde{z}_{i,j,t}$ for a specific location (i,j,t) is computed as follows:

$$\tilde{z}_{i,j,t}^1 = soft\max\left(\frac{q_{i,j,t}K_1^T}{\sqrt{d}}\right)V_1 \tag{20}$$

$$\tilde{z}_{i,j,t}^2 = soft\max\left(\frac{q_{i,j,t}K_2^T}{\sqrt{d}}\right)V_2 \tag{21}$$

$$\tilde{z}_{i,j,t}^3 = soft\max\left(\frac{q_{i,j,t}K_3^T}{\sqrt{d}}\right)V_3 \tag{22}$$

$$\tilde{z}_{i,j,t} = \tilde{z}_{i,j,t}^1 + \tilde{z}_{i,j,t}^2 + \tilde{z}_{i,j,t}^3 \tag{23}$$

where $q_{i,j,t}$ is the corresponding query vector, $K_1, V_1 \in \mathbb{R}^{H \times d}$ is the corresponding key-value matrix along the vertical latitudinal direction, $K_2, V_2 \in \mathbb{R}^{W \times d}$ is the corresponding key-value matrix along the horizontal longitudinal direction, $K_3, V_3 \in \mathbb{R}^{T \times d}$ is the corresponding key-value matrix along the time direction.

II. B. 4) Location coding

Recurrent neural networks process the input sequences one by one, thus ensuring temporal backward and forward order, but the attention mechanism abandons sequential operations due to parallel computing. In the weather prediction task, since this paper applies the attention mechanism to the time axis, the vertical and horizontal directions of space, a three-dimensional tensor is needed to represent the location relationship. Similar to the two-dimensional position encoding in images, this paper uses a learning strategy to learn three sets of position encoding. Here, the dimension of each group of position encoding is set to $d/3$, and d is the dimension of the feature in the attention module. Based on the position coordinates of the input tensor, the three sets of position encoding will be connected together to represent the final position embedding representation.

II. B. 5) Spatial regression networks

The spatial regression network consists of an anti-convolution layer with an activation function. The inverse convolution operation is the opposite of conventional convolution and enables up-sampling of the input data. The spatial regression network then maps the feature map $\left\{Z^{t+1}, Z^{t+2}, \cdots, Z^{t+T_{out}}\right\}$ generated by the decoder into the meteorological state space with greater spatial resolution. After obtaining the prediction results, it is trained by minimizing the mean square error between the predicted and true values, and the corresponding loss function is defined as:

$$L(Y,\hat{Y}) = \frac{\left\|Y-\hat{Y}\right\|^2}{E \times P \times H \times W} \tag{24}$$

where Y is the real meteorological observation sequence, $\hat{Y}$ is the predicted meteorological observation sequence, E is the number of meteorological modes, P is the number of isobaric layers, and H and W denote the number of grids in the longitudinal and latitudinal directions, which are related to the size of the area to be predicted and the spatial resolution.

III. Experimental procedures and analysis of results

III. A. Experimental platform environment construction

The hardware of the experimental platform environment uses an MSI B450M MORTAR MAX (MS-7B89) motherboard, AMD Ryzen 7 5700X 8-core, 16-thread processor, 32GB of DDR4 3600MHZ (16GB+16GB) RAM, a CUDA-enabled NVDIA GeForce RTX3070 GPU and a KIOXIA-EXCERIA G2 SSD 1TB solid state drive.

The software environment uses Windows 10 Professional 64-bit operating system, Python as the main development language and Pycharm as the main IDE. Pytorch framework is used to build the deep learning model, while pandas, numpy and other dependent libraries are used for data processing. The deep learning process is accelerated using the CUDA feature of GPU.

III. B. Analysis of the effect of Kalman filtering algorithms

III. B. 1) Parameter selection

Inversion of atmospheric parameters using the Kalman filter method firstly needs to clarify the real physical process that occurs during the detection process, i.e., the physical process that the optical signal emitted by the lidar interacts with the atmospheric medium in order to produce the measurement results, which is also known as the cloud radar equation. In this paper, the NRLMSISE-00 atmospheric model is chosen as the output a priori state model atmosphere of each major component, and the CIRA-76 model atmosphere is used as a reference to calculate the gravity acceleration of each place.

III. B. 2) Analog simulation

Before analyzing the real detection data of cloud radar, it is necessary to study and evaluate the proposed inversion algorithm in order to minimize or try to eliminate the systematic errors generated during the inversion process. Therefore, this paper will first simulate the overall inversion process of the lidar by using simulated echo data in order to detect and eliminate other factors that may affect the detection and to correct possible errors in the temperature inversion algorithm.

In the lower atmosphere the laser signal scatters mainly with aerosols. At the same time, combined with the hardware characteristics of LIDAR itself, the effective detection altitude range is generally 40-100 km above sea level in the atmospheric space. Without considering the scattering and extinction effects of aerosols on the emitted laser beam, Poisson statistical uncertainty is added to the echo photon data obtained from the simulation with a spatial resolution of 130m.

The key to the Kalman filtering algorithm is to establish an accurate system state model. However, it is difficult to get an accurate description of a real system like the middle atmosphere, and often only an approximate model can be used instead. Therefore, the generating parameter matrices of the standard atmosphere model are also approximated this time to be replaced by an approximate state model, in which the state transfer matrices are all fitted from the standard atmosphere model data. According to the previous research, the approximate model of 4-dimensional state transfer matrix with better effect is selected. In addition to this, the traditional CH integration method is applied in this paper, and the atmospheric temperature at 100 km is selected as the reference temperature. The inversion operation is also carried out while keeping other parameters as well as the introduced error unchanged, in order to compare the difference between it and the Kalman filter algorithm.

III. B. 3) Analysis of results

The inversion data obtained during the simulation are used as the basis for inverting and analyzing the measured echo data of cloud radar using the NRLMSISE-00 atmospheric model as the a priori state temperature information, and the linear Kalman filter and the extended Kalman filter are applied.

The inversion of the cloud radar measured echo photon data at 0600 UT on May 22, 2023 is processed using Kalman filter and improved Kalman filter after deducting the background noise, respectively. The temperature contours measured by the same lidar system at altitudes in the interval of 40-75 km were taken as the real values of temperature. The Kalman filter inversion yields the temperature contours and their deviations from the true values are shown in Figures 3 and 4. And the temperature contours and their deviations from the true values obtained by the improved Kalman filter inversion are shown in Fig. 5 and Fig. 6.

Observing Fig. 3 and Fig. 4, it can be seen that in the practical application, for the altitude interval of 40~75km above sea level, the Kalman filter algorithm can still ensure a certain degree of sensitivity and inversion accuracy, and the atmospheric temperature profile obtained by its inversion basically coincides with the actual temperature profile, and its overall deviation is less than 4.8K. Meanwhile, comparing and observing it with Fig. 5 and Fig. 6, it is easy to find that the improved Kalman filtering shows better sensitivity and accuracy, and its deviation is less than 3.2K overall.

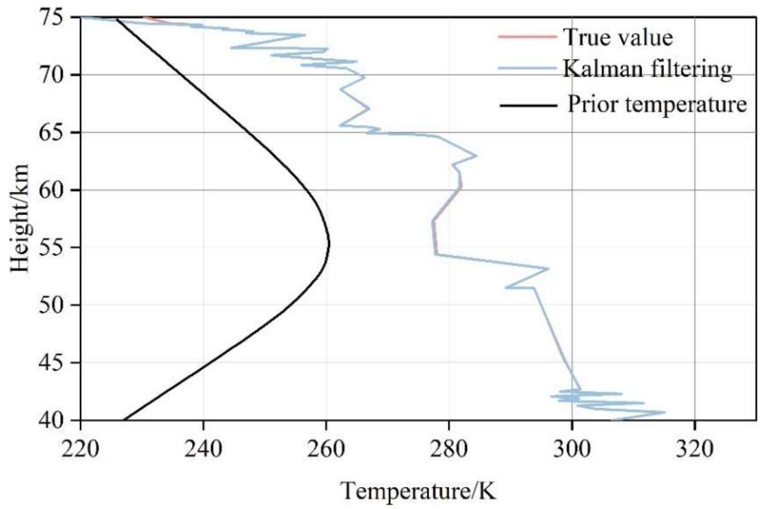

Figure 3: Kalman filter inversion gets the temperature profile

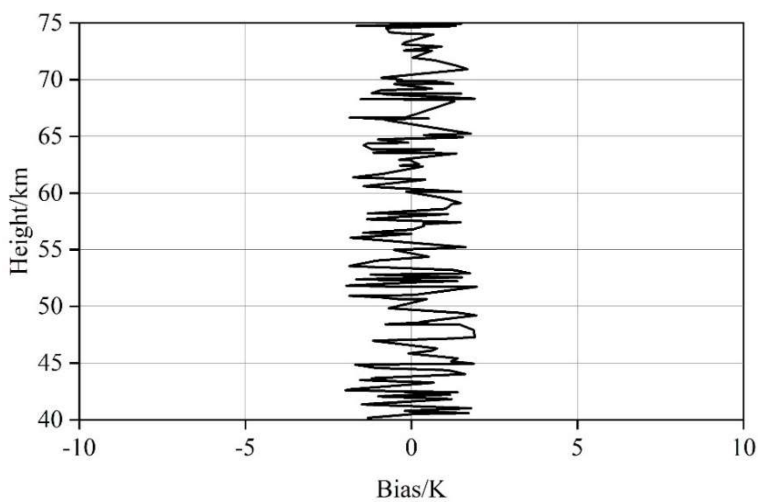

Figure 4: Kalman filter inversion is the deviation of temperature and real value

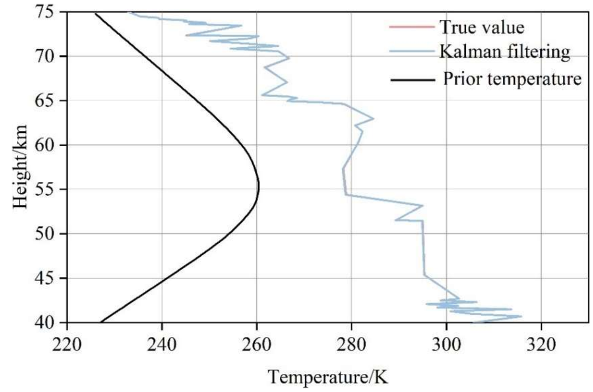

Figure 5: Improved Kalman filter inversion gets the temperature profile

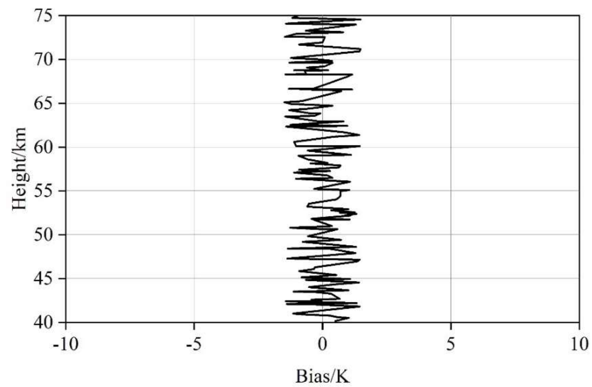

Figure 6: Improve the deviation of the Kalman filter to the temperature and true value

It is evident that there is a significant difference between the model atmospheric temperature, which is the a priori state temperature, and the temperature profile obtained by the inversion, i.e., the state information of the inversion as a whole is mainly derived from the measured information rather than the a priori information. This indicates that the contribution of the a priori information to the inversion is relatively low and is regarded as a reasonably good inversion process.

III. C. Analysis of the effect of the application of meteorological forecasting models

The multimodal fusion weather prediction model is validated and compared with LSTM model and RNN model respectively. The average dew point, average temperature, maximum temperature, minimum temperature, snow depth, whether it rained or not and whether it snowed or not meteorological feature data of the previous day were used as inputs. The loss values of each optimized model are shown in Fig. 7. The model in this paper shows better convergence speed and convergence accuracy.

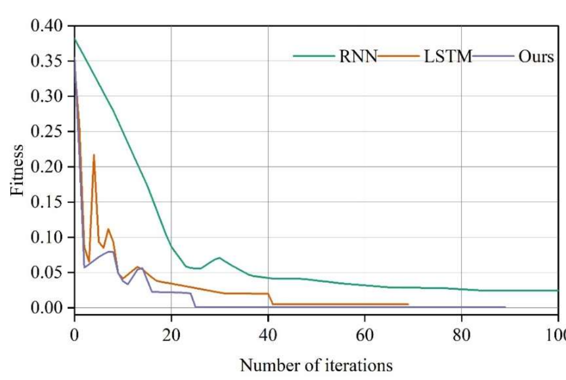

Figure 7: Optimization model loss value

In this paper, the data from May 26, 2023 to September 26, 2029 are selected for the comparative demonstration of the prediction results, and the actual values are compared with the model predictions, and the prediction results are shown in Fig. 8. Compared with the LSTM model and the RNN model, the prediction results of the multimodal fusion weather prediction model are closest to the real values.

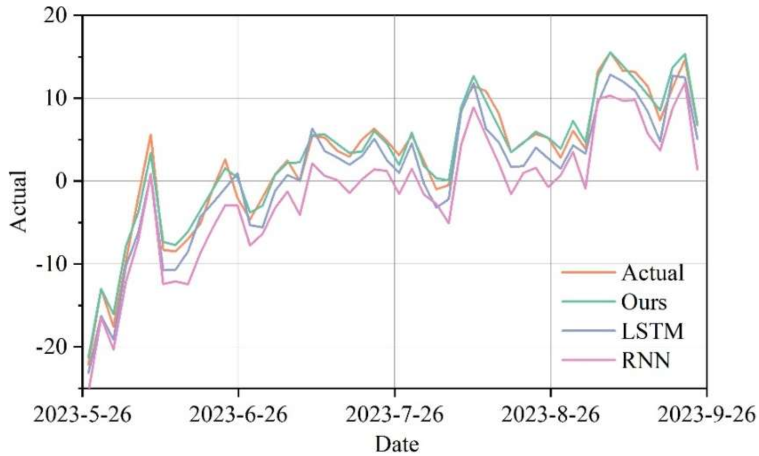

Figure 8: Optimal model prediction results

The RMSE, MSE, MAPE and R^2 values of the tested multimodal fusion weather prediction model and the other two models are shown in Figure 9. The R^2 values of the three models are 0.9635, 0.8624, and 0.7881, respectively, in which the R^2 value of the model in this paper is close to 1, i.e., the model has a high degree of fit. The RMSE, MAPE and MSE of the weather prediction model with multimodal fusion are 2.6483, 0.0229 and 6.1827, respectively, which are lower than those of the LSTM and RNN models. It shows that individual models have certain limitations and cannot adequately capture the characteristics and trends of the data, thus failing to obtain the optimal prediction results. The model in this paper has a higher optimization seeking advantage, which can better improve the model prediction accuracy.

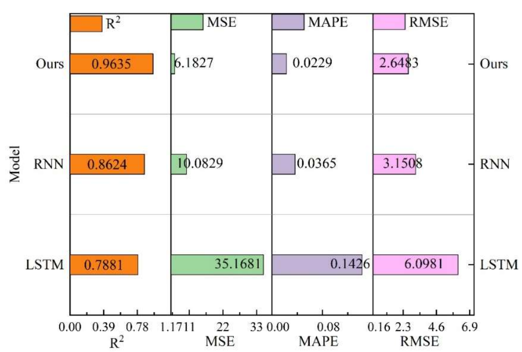

Figure 9: Forecast evaluation of each optimization model

IV. Conclusion

The improved Kalman filter algorithm shows high accuracy in temperature inversion, and the overall deviation is less than 3.2K for the temperature prediction in the interval of 40-75km above sea level, which indicates that the algorithm has a good inversion capability. Compared with LSTM and RNN models, the weather prediction model based on multimodal fusion has significant advantages in prediction accuracy. The experimental results show that the R^2 value of the model reaches 0.9635, indicating that it has a very high degree of fit. In addition, the RMSE of the model is 2.6483, the MAPE is 0.0229, and the MSE is 6.1827, which are better than the traditional model. The multimodal data fusion further improves the accuracy of weather prediction, indicating that the intelligent weather prediction model proposed in this paper has a better application prospect, which can effectively respond to complex weather changes and provide more accurate weather forecasting services.

Acknowledgement

This work was supported by Shanxi Province Meteorological Surface Project: Research on cloud physics feature inversion in Shanxi Province based on cloud radar (SXKMSDW20246752).

References

[1] Biswas, M., Dhoom, T., & Barua, S. (2018). Weather forecast prediction: an integrated approach for analyzing and measuring weather data. International Journal of Computer Applications, 182(34), 20-24.

[2] Scher, S., & Messori, G. (2018). Predicting weather forecast uncertainty with machine learning. Quarterly Journal of the Royal Meteorological Society, 144(717), 2830-2841.

[3] Holmstrom, M., Liu, D., & Vo, C. (2016). Machine learning applied to weather forecasting. Meteorol. Appl, 10(1), 1-5.

[4] Price, I., Sanchez-Gonzalez, A., Alet, F., Andersson, T. R., El-Kadi, A., Masters, D., ... & Willson, M. (2025). Probabilistic weather forecasting with machine learning. Nature, 637(8044), 84-90.

[5] Meenal, R., Binu, D., Ramya, K. C., Michael, P. A., Vinoth Kumar, K., Rajasekaran, E., & Sangeetha, B. (2022). Weather forecasting for renewable energy system: a review. Archives of Computational Methods in Engineering, 29(5), 2875-2891.

[6] Fathi, M., Haghi Kashani, M., Jameii, S. M., & Mahdipour, E. (2022). Big data analytics in weather forecasting: A systematic review. Archives of Computational Methods in Engineering, 29(2), 1247-1275.

[7] Abhishek, K., Singh, M. P., Ghosh, S., & Anand, A. (2012). Weather forecasting model using artificial neural network. Procedia Technology, 4, 311-318.

[8] Conti, S. (2024). Artificial intelligence for weather forecasting. Nature Reviews Electrical Engineering, 1(1), 8-8.

[9] Rasp, S., Dueben, P. D., Scher, S., Weyn, J. A., Mouatadid, S., & Thuerey, N. (2020). WeatherBench: a benchmark data set for data-driven weather forecasting. Journal of Advances in Modeling Earth Systems, 12(11), e2020MS002203.

[10] Bühl, J., Seifert, P., Radenz, M., Baars, H., & Ansmann, A. (2019). Ice crystal number concentration from lidar, cloud radar and radar wind profiler measurements. Atmospheric Measurement Techniques, 12(12), 6601-6617.

[11] Kalesse, H., Szyrmer, W., Kneifel, S., Kollias, P., & Luke, E. (2016). Fingerprints of a riming event on cloud radar Doppler spectra: observations and modeling. Atmospheric Chemistry and Physics, 16(5), 2997-3012.

[12] Kalesse-Los, H., Schimmel, W., Luke, E., & Seifert, P. (2022). Evaluating cloud liquid detection against Cloudnet using cloud radar Doppler spectra in a pre-trained artificial neural network. Atmospheric Measurement Techniques, 15(2), 279-295.

[13] Lovén, L., Karsisto, V., Järvinen, H., Sillanpää, M. J., Leppänen, T., Peltonen, E., ... & Riekki, J. (2019). Mobile road weather sensor calibration by sensor fusion and linear mixed models. PloS one, 14(2), e0211702.

[14] Djordjevic, M., & Dankovic, D. (2019). A smart weather station based on sensor technology. Facta Universitatis, Series: Electronics and Energetics, 32(2), 195-210.

[15] Pujahari, R. M., Yadav, S. P., & Khan, R. (2022). Intelligent farming system through weather forecast support and crop production. In Application of Machine Learning in Agriculture (pp. 113-130). Academic Press.

[16] Mestre, G., Ruano, A., Duarte, H., Silva, S., Khosravani, H., Pesteh, S., ... & Horta, R. (2015). An intelligent weather station. Sensors, 15(12), 31005-31022.

[17] Xuan, Y., Kan, D. A. I., & Yuejian, Z. H. U. (2022). Progress and challenges of deep learning techniques in intelligent grid weather forecasting. Acta Meteorologica Sinica, 80(5), 649-667.

[18] Abazari, A., Soleymani, M. M., Kamwa, I., Babaei, M., Ghafouri, M., Muyeen, S. M., & Foley, A. M. (2021). A reliable and cost-effective planning framework of rural area hybrid system considering intelligent weather forecasting. Energy Reports, 7, 5647-5666.

[19] Yuan, Y., Fu, F., Li, Y., Xing, Y., Wang, L., Zheng, H., & Ye, W. (2023). Research and Application of Intelligent Weather Push Model Based on Travel Forecast and 5G Message. Atmosphere, 14(11), 1658.

[20] Ukhurebor, K. E., Adetunji, C. O., Olugbemi, O. T., Nwankwo, W., Olayinka, A. S., Umezuruike, C., & Hefft, D. I. (2022). Precision agriculture: Weather forecasting for future farming. In Ai, edge and iot-based smart agriculture (pp. 101-121). Academic Press.

[21] Chao, Z. (2023). Machine learning-based intelligent weather modification forecast in smart city potential area. Computer Science and Information Systems, 20(2), 631-656.

[22] Bharti, G. K., Ranjan, A., Bharat, A., & Yadav, S. (2023). Design and development of an efficient and intelligent weather forecasting app. In Recent Developments in Electronics and Communication Systems (pp. 353-358). IOS Press.

[23] Rudrappa, G., & Vijapur, N. (2019). Intelligent Methods Used for Obtaining Weather Derivatives: A Review. Engineering and Applied Sciences., 4(6), 144-148.

[24] Ezhilarasi, V., Selvamuthukumaran, S., & Srinivasan, N. (2024). 22 Intelligent Weather Forecasting Farming Through Using Deep Learning Techniques for Enhancing Crop Productivity. Intelligent Systems and Sustainable Computational Models: Concepts, Architecture, and Practical Applications, 339.

[25] Xiao Tian Wang,Ze Zheng Zhang,Jie Sheng Wang,Song Bo Zhang & Xun Liu. (2024). Lithium-ion Battery State of Charge Estimation Model Based on Kalman Filtering Algorithm and Equivalent Circuit. Engineering Letters,32(7),

[26] Remzilnan. (2024). An Improved Model Predictive Current Control of BLDC Motor With a Novel Adaptive Extended Kalman Filter–Based Back EMF Estimator and a New Commutation Duration Approach for Electrical Vehicle. International Journal of Circuit Theory and Applications,53(2),1135-1150.

[27] Lingtao Wu,Wenhao Guo,Yuben Tang,Youming Sun & Tuanfa Qin. (2024). Remaining Useful Life Prediction of Lithium-Ion Batteries Based on Neural Network and Adaptive Unscented Kalman Filter. Electronics,13(13),2619-2619.

[28] Minseo Park & Jangmin Oh. (2024). Enhancing E-Commerce Recommendation Systems with Multiple Item Purchase Data: A Bidirectional Encoder Representations from Transformers-Based Approach. Applied Sciences,14(16),7255-7255.